C. R. Chimie 18 (2015) 954–959

Contents lists available at ScienceDirect

Comptes Rendus Chimie

www.sciencedirect.com

Full paper/Mémoire

Theoretical study of the optical and charge transport properties of star-shaped molecules with 1,3,5-triazine-core derivatives as organic light-emitting and organic solar cells materials

Ruifa Jin

Inner Mongolia Key Laboratory of Photoelectric Functional Materials, College of Chemistry and Chemical Engineering, Chifeng University, Chifeng 024000, PR China

ARTICLE INFO

Article history:
Received 6 March 2015
Accepted after revision 28 May 2015
Available online 21 August 2015

Keywords:
Star-shaped molecules
1,3,5-Triazine derivatives
Electronic and optical properties
Charge transport property
Organic electronics

ABSTRACT

A series of D–π–A star-shaped molecules has been investigated theoretically by using density functional theory (DFT) to reveal their optical, electronic, and charge transport properties for applications in organic light-emitting diodes (OLEDs) and organic solar cells (OSCs). The calculated results show that their optical, electronic, and charge transport properties are affected by the different end groups and π-bridges. Our results reveal that the molecules under investigation can serve as OSCs donor materials and/or luminescent materials for OLEDs. In addition, all molecules are expected to be promising candidates for hole- and electron-transport materials. On the basis of the obtained results, we propose a rational way for the design of multifunctional materials for OLEDs and OSCs applications.

1. Introduction

The development of organic electronics, including organic solar cells (OSCs) and organic light-emitting diodes (OLEDs), has received a significant amount of attention in recent years because of their light weight, of their potential low cost, because they can be used to make large-area flexible and transparent panels, and because the fabrication of the devices is easy [1–7]. Especially, small molecule-based organic electroactive molecules are of increasing importance for their optoelectronic applications in OSCs and OLEDs because they exhibit good light absorption, light-emitting, and charge-carrier transport properties. It is believed that small molecule-based organic electronics are promising for their commercial application in the future. Although enormous progresses have been made recently in the research and the development of new materials, the lower efficiency of small molecule-based organic electronics materials is still the main obstacle to their application. It is therefore necessary to develop novel high-efficiency multifunctional organic materials. They are capable of transporting charge in addition to serving as efficient light-absorption materials in OSCs as well as emitters with excellent performance in OLEDs, respectively [8–13]. Theoretical studies on multifunctional organic materials may provide useful insights into the understanding of the nature of the molecules [14–17]. Among the organic materials, star-shaped conjugated materials have become the most efficient strategy used in the design and synthesis of multifunctional OLEDs and OSCs materials [18–22]. The formation of an ordered, long-range, and coplanar *p*–*p* stacking can be prevented by the increased steric hindrance of star-shaped conjugated molecules. This may lead them to be good candidates as charge transport materials. At the same time, the absorption and emission spectra of these materials can be tuned effectively through adjusting the core and arm units, and π-conjugated bridge units or length when applied in organic electronics [23]. Recently, multifunctional star-shaped molecules with

Email address: Ruifajin@163.com.

http://dx.doi.org/10.1016/j.crci.2015.05.021
1631-0748/

triazine core and various bithiophene branches have been reported for light-emitting materials in OLEDs, donor materials in OSCs, and active channels in organic field-effect transistors (OFETs) [24].

In this contribution, we designed a series of star-shaped D–π–A molecules with 1,3,5-triazine (TZ) as the core, aromatic derivatives as end groups, and thiophene or furan π-bridges for applications in organic electronics (Scheme 1). Furthermore, we explored the optical and electronic properties of the molecules with the aim to get a further insight into the relationship between topologic structure and optical as well as electronic properties. This provides a method for the rational design of good candidates for OLEDs and OSCs materials.

2. Computational methods

All calculations were carried out with the aid of the Gaussian 09 package [25]. The geometries of the compounds under investigation in ground states (S_0) were optimized using the B3LYP method. The corresponding geometries in the first excited singlet state (S_1) were optimized using TD-B3LYP. All geometry optimizations were performed using the 6-31G(*d,p*) basis set. The harmonic vibrational frequency calculations using the same methods as for the geometry optimizations were used to ascertain the presence of a local minimum. The absorption and fluorescent properties of the compounds under investigation were predicted using the TD-B3LYP/6-31+G(*d,p*) based on the optimized S_0 and S_1 geometries, respectively. To investigate the influence of solvents on the optical properties for the S_0 and S_1 states of the molecular systems in toluene as a solvent (dielectric constant: 2.374), we performed polarized continuum model (PCM) [26] calculations at the TD-DFT level.

The charge transfer rate can be described by the Marcus theory [27,28]:

$$K = \left(V^2/\hbar\right)\left(\pi/\lambda k_B T\right)^{1/2}\exp\left(-\lambda/4k_B T\right) \quad (1)$$

where k_B is the Boltzmann constant, T is the temperature, λ corresponds to the reorganization energy, and V represents the intermolecular transfer integral. It can be seen from Eq. (1) that the λ and V values have a dominant impact on the charge transfer rate, especially the former. In order to predict V, crystal data are required. However, the investigated molecules may be noncrystal. Thus, in this paper, we focus on the reorganization energies λ to investigate their charge transport properties. The reorganization energy λ is further divided into two parts, external and internal reorganization energies [29]. We only study the internal reorganization energy because the external reorganization energy is quite complicated to evaluate at this stage. Furthermore, the computed values of the external reorganization energy in pure organic condensed phases are much smaller than their internal reorganization energy and can be neglected [30–32]. In addition, there is a clear correlation between internal reorganization energy and charge transfer rate in the literature [33,34]. Therefore, we study exclusively the internal reorganization energy in this work. Hence, the electron (λ_e) and hole (λ_h) reorganization energy can be calculated by Eqs. (2) and (3) [35]:

$$\lambda_e = \left(E_-^0 - E_-^-\right) + \left(E_0^- - E_0^0\right) \quad (2)$$

$$\lambda_h = \left(E_+^0 - E_+^+\right) + \left(E_0^+ - E_0^0\right) \quad (3)$$

where $E_0^+(E_0^-)$ is the energy of the cationic (anionic) states at the geometry of the optimized neutral molecule. $E_+^+(E_-^-)$ is the energy of the cationic (anionic) states with the optimized cationic (anionic) structures. $E_0^+(E_0^-)$ is the energy of the neutral states at the cationic (anionic) structures. E_0^0 is the energy of the neutral molecule in the ground state. Furthermore, in order to compare with the results reported in literature [36,37], the λ_e and λ_h values of the molecules were predicted at the B3LYP/6-31G(*d,p*) level.

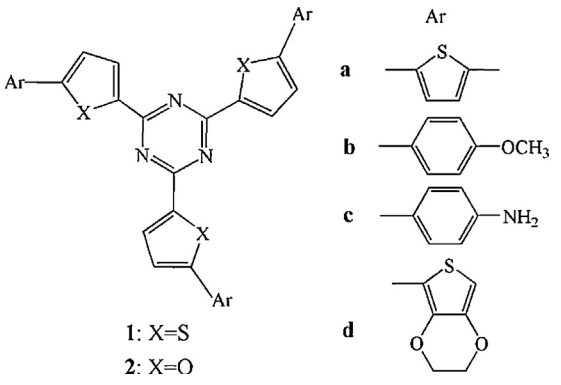

Scheme 1. Molecular structures of the investigated molecules.

3. Results and discussion

3.1. Frontier molecular orbitals

The qualitative frontier molecular orbitals (FMOs), including the highest occupied molecular orbital (HOMO) and the lowest unoccupied molecular orbital (LUMO) of the investigated molecules (**1a–d** and **2a–d**), are shown in Fig. 1. The total and partial densities of states (TDOS and PDOS) on each fragment of **1a–d** and **2a–d** around the HOMO–LUMO gaps were calculated based on the current level of theory. The FMOs energies E_{HOMO} and E_{LUMO}, HOMO–LUMO gaps E_g, and the contributions of individual fragments (in %) to the FMOs of **1a–d** and **2a–d** are given in Table 1. The distribution patterns and contributions of individual fragments (in %) of HOMOs – 1, HOMOs – 2, and LUMOs + 1 for the investigated molecules are given in Fig. SI and Table SI in the Supplementary data, respectively. The FMOs of **1a–d** and **2a–d** show π characteristics as visualized in Fig. 1. The HOMOs are mainly localized on the aromatic end groups (**AR**) and conjugate π-bridge fragments (**CB**) with only minor but nonzero contributions from the **TZ** fragments. On the contrary, the LUMOs mainly reside at the **TZ**, **CB**, and **AR** fragments of two arms. These results reveal that the different π-bridge units and end groups have obvious effects on the distribution of FMOs for the compounds under investigation. The distribution

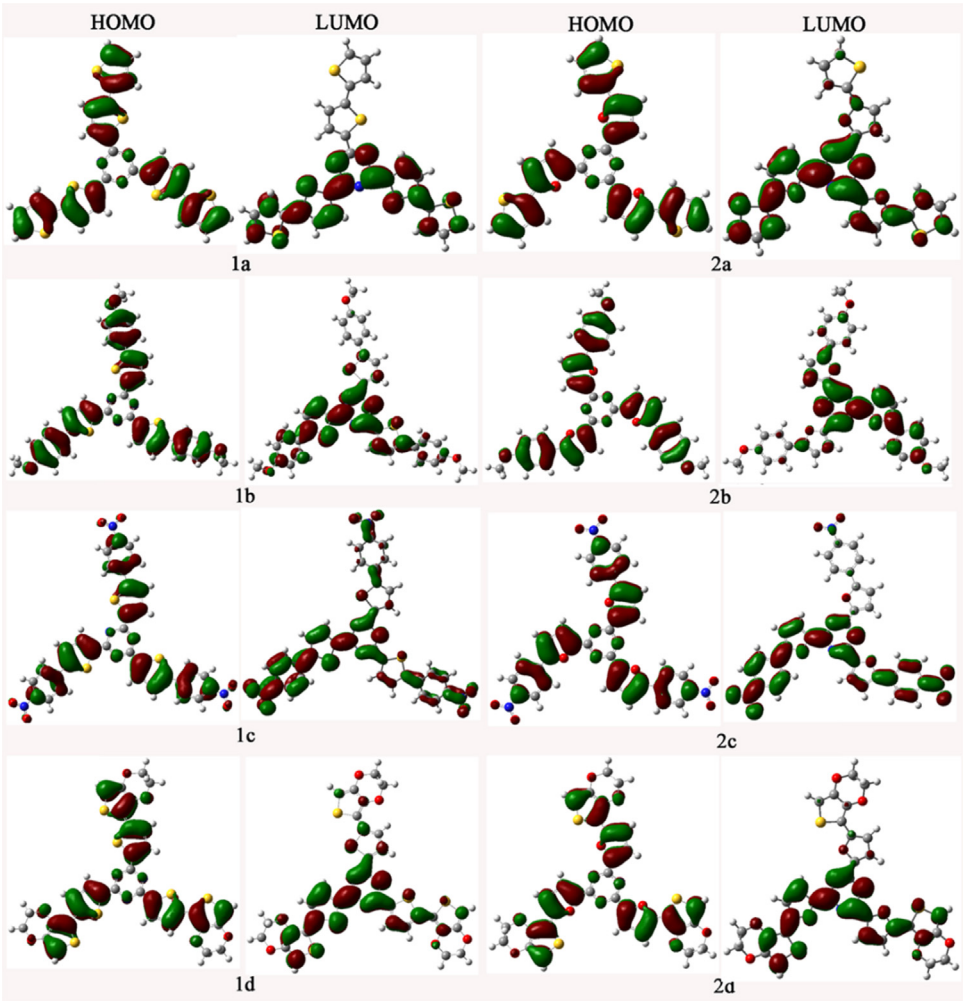

Fig. 1. (Color online). The electronic density contours of the frontier orbitals for the investigated molecules at the B3LYP/6-31G(*d*,*p*) level.

patterns of the FMOs of the compounds under investigation provide a remarkable signature for the intramolecular charge transfer (ICT) character of the vertical $S_0 \rightarrow S_1$ transition. The results displayed in Table 1 show that the contributions of the **TZ** fragments to LUMOs are increased, while the corresponding contributions of the **CB** fragments are decreased compared with those of to HOMOs, respectively. The contributions of **AR** fragments to LUMOs are decreased, except the corresponding contributions of **1c** and **2c**, which are increased compared with those of HOMOs, respectively. This indicates that the excitation of the electron from the HOMOs to LUMOs leads the electronic density to flow mainly from the **AR** and **CB** fragments to the **TZ** fragments for **1a**, **1b**, **1d**, **2a**, **2b**, and **2d**,

Table 1
The FMOs energies E_{HOMO} and E_{LUMO}, HOMO–LUMO gaps E_g (all in eV), and HOMOs and LUMOs contributions (%) of the compounds under investigation at the B3LYP/6-31G(*d*,*p*) level.

Species	HOMO				LUMO				E_g
	E_{HOMO}	TZ	CB	AR	E_{LUMO}	TZ	CB	AR	
1a	−5.595	2.8	50.8	46.4	−2.167	37.1	42.2	20.5	3.428
1b	−5.386	2.6	46.7	50.7	−1.822	42.3	44.5	13.2	3.364
1c	−6.602	3.6	65.4	31.0	−3.044	21.5	27.3	51.2	3.558
1d	−5.164	2.7	47.2	50.1	−1.872	35.9	41.2	22.9	3.292
2a	−5.461	3.2	53.9	43.0	−1.932	42.1	34.1	23.8	3.528
2b	−5.187	3.0	50.5	46.5	−1.603	47.0	36.2	16.8	3.584
2c	−6.453	3.7	64.5	31.8	−2.985	20.7	20.1	59.3	3.469
2d	−5.034	3.0	49.9	47.1	−1.614	41.1	33.5	25.4	3.420

TZ: 1,3,5-triazine moieties; CB: conjugate bridge moieties; AR: aromatic moieties.

while the corresponding electronic density flows mainly from the **CB** fragments to the **TZ** and **AR** fragments for **1c** and **2c**. The percentages of charge transfer are the differences between the contributions of the fragments for LUMOs and the corresponding contributions for HOMOs in the compounds under investigation. The percentages of charge transfer from **AR** and **CB** fragments to **TZ** fragments are 33.2–39.7% for **1a**, **1b**, **1d**, **2a**, **2b**, and **2d**. The corresponding percentages of charge transfer from the **CB** fragments to **TZ** and **AR** fragments for **1c** and **2c** are 38.1 and 44.4%, respectively. The results displayed in Table 1 reveal that the **AR** and **CB** fragments serve as donors and the **TZ** fragments serve as acceptors for **1a**, **1b**, **1d**, **2a**, **2b**, and **2d**. The **CB** fragments serve as donors and the **TZ** and **AR** fragments serve as acceptors for **1c** and **2c**. Furthermore, the photophysical properties of ICT are well known and highly dependent on the electron donor/acceptor strength [38,39]. The introduction of different donor (acceptor) groups strengthens the electron-donating (-withdrawing) abilities of donors (acceptors). Therefore, the ICT transition in the star-shaped D–π–A molecules becomes much easier after having introduced different donor (acceptor) groups, resulting in the large bathochromic shift in their absorption and fluorescence spectra.

Another way to understand the influence of the optical and electronic properties is to analyze the E_{HOMO}, E_{LUMO}, and E_g values. Inspection of Table 1 reveals that both the E_{HOMO} and E_{LUMO} values of **1b**, **1d**, **2a**, **2b**, and **2d** increase, while the corresponding values of **1c** and **2c** decrease compared with those of **1a**. The E_{HOMO} values are in the order **2d** > **1d** > **2b** > **1b** > **2a** > **1a** > **2c** > **1c**. The sequence of E_{LUMO} is **2b** > **2d** > **1b** > **1d** > **2a** > **1a** > **1c** > **2c**. Thus, the E_g values of **1c**, **2a**, **2b**, and **2c** increase, while the corresponding value of **1b**, **1d**, and **2d** decrease compared with that of **1a**. The E_g values of **1a–d** are in the order **1c** > **1a** > **1b** > **1d**, while the corresponding E_g values of **2a–d** are in the order **2b** > **2a** > **2c** > **2d**. The E_g values of **1d** and **2d** are smaller than those of **1a–c** and **2a–c**, respectively. It suggests that the 2,3-dihydrothieno[3,4-*b*][1,4]dioxine end group is responsible for the smaller E_g value. For the molecules with thiophene and furan π-bridges, the E_g values of molecules with 2,3-dihydrothieno[3,4-*b*][1,4]dioxine end groups are smaller than that of the corresponding molecules with thiophene, anisole, and 1-nitrobenzene end groups. It reveals that the 2,3-dihydrothieno[3,4-*b*][1,4]dioxine end group can decrease the E_g value in comparison with the thiophene, anisole, and 4-nitrobenzene end groups when the π-bridges are the same.

It is well known that [6,6]-phenyl-C_{61}-butyric acid methyl ester (PCBM) and its derivatives bisPCBM and PC70BM are excellent acceptors for organic solar cells [40–43]. Therefore, we chose these three fullerene derivatives as acceptors in our work. The FMOs energies E_{HOMO} and E_{LUMO} are listed in Table 2. Comparing the results shown in Table 1 with those in Table 2, one can find that the E_{LUMO} values of **1a–d** and **2a–d** are higher than those of PCBM, bisPCBM, and PC70BM, respectively, except that the corresponding value of **1c** is slightly lower than that of bisPCBM. The differences between the E_{HOMO} of **1a–d** and **2a–d** and the E_{LUMO} of PCBM, bisPCBM, and PC70BM are larger than 1.917, 2.013, and 1.952 eV, respectively. These results imply that the designed molecules can provide better matches of FMOs to PCBM, bisPCBM, and PC70BM, except that **1c** provides better matches of FMOs to PCBM and PC70BM. Therefore, different π-bridges and end groups can tune the FMOs of derivatives more suitable to PCBM, bisPCBM, and PC70BM.

Table 2
Calculated E_{HOMO} and E_{LUMO} (all in eV) of PCBM, bisPCBM, and PC70BM at the B3LYP/6-31G(*d*,*p*) level.

Species	E_{HOMO}	E_{LUMO}
PCBM	−5.670	−3.117
bisPCBM	−5.474	−3.021
PC70BM	−5.613	−3.082

3.2. Absorption and fluorescence spectra

The absorption λ_{abs} and fluorescence λ_{fl} wavelengths, main assignments, and the oscillator strength *f* for the most relevant singlet excited states of **1a–d** and **2a–d** are listed in Tables 3 and 4, respectively. The λ_{abs} value of **1a** is equal to that of the experimental result, while the corresponding value of λ_{fl} is in agreement with the experimental results [24]; the deviation is 14 nm. The Stokes shift of **1a** is 52 nm, which is comparable to the experimental 66 nm. Thus, this result credits to the computational approach, so appropriate electronic transition energies can be predicted at these levels for this kind of system. For the absorption spectra, the HOMOs → LUMOs transitions play a dominant role for **1a–d** and **2a–d**. Furthermore, the absorptions of **1b**, **1c**, **2a**, **2c**, and **2d** also originate from the HOMOs − 1 → LUMOs transitions. The transition of **1a** and **2c** also corresponds to HOMOs → LUMOs + 1 transitions. The results presented in Table 3 show that the λ_{abs} of **1a–c** and **2a–d** have slight hypsochromic shifts 15, 15, 10, 16, and 8 nm compared with that of the parent compound **1a**, respectively. The λ_{abs} values of **1d** and **2d** show slight bathochromic shifts (17 and 3 nm) compared with that of **1a**. Moreover, **1a–d** and **2b–d**

Table 3
Longest wavelength of absorption spectrum λ_{abs}, corresponding oscillator strength *f*, and main assignments (coefficient) for the compounds under investigation at the TD-B3LYP/6-31G(*d*,*p*)//B3LYP/6-31G(*d*,*p*) level, along with available experimental data.

Species	λ_{abs}	*f*	Assignment
1a	408	0.24	H → L (0.57)
			H → L + 1 (0.37)
1b	393	0.88	H → L (0.68)
			H-1 → L (0.11)
1c	393	1.36	H → L (0.55)
			H-1 → L (0.28)
1d	425	0.37	H → L (0.69)
2a	398	0.16	H → L (0.65)
			H-1 → L (0.18)
			H-2 → L + 1 (−0.19)
2b	392	0.45	H → L (0.70)
2c	400	1.06	H → L (0.48)
			H → L + 1 (0.42)
			H-1 → L (−0.20)
2d	411	0.26	H → L (0.67)
			H-1 → L (0.13)
Exp[a]	394		

[a] The experimental λ_{abs} values of **1a** in CH_2Cl_2 were taken from Ref. [24].

Table 4
The strongest fluorescence wavelengths λ_{fl} (in nm), the oscillator strength *f*, and main assignments (coefficient) of the compounds under investigation at the TD-B3LYP/6-31G(*d*,*p*)//TD-B3LYP/6-31(*d*,*p*) level, along with available experimental data.

Species	λ_{fl}	*f*	Assignment
1a	460	0.31	H ← L (0.70)
1b	438	0.46	H–1 ← L (0.70)
1c	447	0.24	H–1 ← L (0.68)
			H–2 ← L (0.16)
1d	473	0.32	H–1 ← L (0.70)
2a	432	0.48	H–1 ← L (0.68)
			H–2 ← L (0.14)
2b	422	0.74	H–1 ← L (0.67)
			H–2 ← L (0.21)
2c	446	0.24	H–1 ← L (0.68)
			H–2 ← L (0.12)
2d	447	0.50	H–1 ← L (0.69)
Exp[a]	460		

[a] The experimental λ_{fl} of **1a** in CH_2Cl_2 were taken from Ref. [24].

have larger oscillator strengths than that of **1a**. The *f* value **2a** is slightly less than of **1a**. The oscillator strength for an electronic transition is proportional to the transition moment [44]. In general, larger oscillator strength corresponds to a larger experimental absorption coefficient or a stronger fluorescence intensity. This indicates that **1a**–**d** and **2a**–**d** show larger absorption intensity than that of **1a**, except for **2a**. It suggests that the molecules under investigation could be used as solar cell material with intense absorption spectra.

For the fluorescence spectra, the LUMOs ← HOMOs excitation plays a dominant role for **1a**, while the fluorescence of **1b**–**d** and **2a**–**d** mainly arises from HOMOs – 1 ← LUMOs. Furthermore, the fluorescence of **1c** and **2a**–**d** also originates from the HOMOs – 2 → LUMOs transitions. As shown in Table 4, the λ_{fl} values of **1b**, **1c**, and **2a**–**d** show hypsochromic shifts 22, 13, 28, 38, 14, and 13 nm compared with that of **1a**, respectively. The Stokes shifts of **1a**–**c** and **2a**–**d** are 52, 45, 54, 34, 30, 46, and 36 nm, respectively. The λ_{fl} of **1d** has a bathochromic shift of 13 nm compared with that of the parent compound **1a**. Furthermore, the *f* values of **1b**, **1d**, **2a**, **2b**, and **2d** are larger than that of **1a**, except that the corresponding value of **1c** and **2c** is slightly less than that of **1a**, corresponding to strong fluorescence spectra. This implies that **1a**–**d** and **2a**–**d** have large fluorescent intensity and they are promising luminescent materials for OLEDs.

3.3. Reorganization energy

The calculated reorganization energies for hole and electron are listed in Table 5. It is well known that, the lower the reorganization energy values, the higher the charge transfer rate [10]. The results displayed in Table 4 show that the λ_h values of **1a**–**d** and **2a**–**d** (0.101–0.224 eV) are much smaller than that of *N*,*N*′-diphenyl-*N*,*N*′-bis(3-methlphenyl)-1,1(-biphenyl)-4,4′-diamine (TPD), which is a typical hole transport material (λ_h = 0.290 eV) [36]. It indicates that the hole-transfer rates of **1a**–**d** and **2a**–**d** may be higher than that of TPD. On the other hand, the calculated λ_e values of **1a**–**d** and **2a**–**d** (0.170–0.267 eV) are smaller than that of tris(8-hydroxyquinolinato)aluminium(III) (Alq3) (λ_e = 0.276 eV), a typical electron-transport material [37]. It suggests that their electron transfer rates might be lower than that of Alq3. The λ_h values are predicted in the order **1c** < **1a** < **1d** < **1b** for **1a**–**1d** and **2c** < **2a** < **2b** < **2d** for **2a**–**d**, respectively. This shows that the thiophene and 4-nitrobenzene end groups lead to the increase of hole-transfer rates for molecules with thiophene and furan π-bridges. For λ_e, the prediction of λ_e values is in the sequence **1a** < **1d** < **1c** < **1b** for **1a**–**1d** and **2c** < **2a** < **2d** < **2b** for **2a**–**d**, respectively. This shows that the introduction of the anisole end group results in a decrease of charger transfer rates for molecules with thiophene and furan π-bridges. Moreover, the difference between λ_e and λ_h values for **1a**–**d** and **2a**–**d** are in the region of 0.043–0.081 eV, showing that they have better equilibrium properties for electron and hole transport. Therefore, these molecules are potential ambipolar charge transport materials (electron and hole) under the proper operating conditions for OLEDs and OSCs from the standpoint of the smaller reorganization energy.

Table 5
Calculated molecular λ_e and λ_h (all in eV) of the compounds under investigation at the B3LYP/6-31G(*d*,*p*) level.

Species	λ_h	λ_e
1a	0.159	0.196
1b	0.224	0.267
1c	0.152	0.227
1d	0.166	0.214
2a	0.123	0.190
2b	0.153	0.234
2c	0.101	0.170
2d	0.158	0.229

4. Conclusions

In this paper, a series of D–π–A star-shaped small molecules with 1,3,5-triazine as the core, aromatic derivatives as end groups, and thiophene or furan π-bridges have been systematically investigated for OLEDs and OSCs applications. Analyses using FMO and local density of states methods evidenced that the vertical electronic transitions of absorption and emission are characterized as intramolecular charge transfer (ICT). The calculated results show that their optical, electronic, and charge transport properties are affected by the different end groups and π-bridges. The designed molecules can provide better matches of FMOs to PCBM, bisPCBM, and PC70BM except for **1c**. Our results reveal that the molecules under investigation, except for **1c**, can serve as OSCs donor materials with intense absorption spectra as well as luminescent materials for OLEDs, whereas **1c** can be made a luminescent material for OLEDs only. In addition, they are expected to be promising candidates for hole- and electron-transport materials. Furthermore, they have better hole- and electron-transporting balance and can act as nice ambipolar materials. On the basis of our results, we proposed a rational way for the design of charge transport and luminescent materials for OLEDs as well as donor materials for OSCs simultaneously.

Acknowledgements

Financial supports from the Research Program of Sciences at Universities of Inner Mongolia Autonomous Region (No. NJZZ235) and the Natural Science Foundation of Inner Mongolia Autonomous Region (No. 2015MS0201) are gratefully acknowledged.

Appendix A. Supplementary data

Supplementary data associated with this article can be found, in the online version, at http://dx.doi.org/10.1016/j.crci.2015.05.021.

References

[1] A.C. Grimsdale, K.L. Chan, R.E. Martin, P.G. Jokisz, A.B. Holmes, Chem. Rev. 109 (2009) 897–1091.
[2] B. Minaev, G. Baryshnikov, H. Agren, Phys. Chem. Chem. Phys. 16 (2014) 1719–1758.
[3] J. Cao, X. Du, S. Chen, Z. Xiao, L. Ding, Phys. Chem. Chem. Phys. 16 (2014) 3512–3514.
[4] Y. Zhu, Z. Yuan, W. Cui, Z. Wu, Q. Sun, S. Wang, Z. Kang, B. Sun, J. Mater. Chem. A 2 (2014) 1436–1442.
[5] B. Walker, C. Kim, T.Q. Nguyen, Chem. Mater. 23 (2011) 470–482.
[6] N.F. Montcada, B. Pelado, A. Viterisi, J. Albero, J. Coro, P.D.L. Cruz, F. Langa, E. Palomares, Org. Electron 14 (2013) 2826–2832.
[7] X. Li, W. Choy, L. Huo, F. Xie, W. Sha, B. Ding, X. Guo, Y. Li, J. Hou, J. You, Y. Yang, Adv. Mater. 24 (2012) 3046–3052.
[8] J. Lu, P.F. Xia, P.K. Lo, Y. Tao, M.S. Wong, Chem. Mater. 18 (2006) 6194–6230.
[9] L. Han, C. Wang, A. Ren, Y. Liu, P. Liu, J. Mol. Sci. 29 (2013) 146–151.
[10] X.K. Liu, C.J. Zheng, J. Xiao, J. Ye, C.L. Liu, S.D. Wang, W.M. Zhao, X.H. Zhang, Phys. Chem. Chem. Phys. 14 (2012) 14255–14261.
[11] D. Sahu, C.H. Tsai, H.Y. Wei, K.C. Ho, F.C. Chang, C.W. Chu, J. Mater. Chem. 22 (2012) 7945–7953.
[12] J. Kwon, M.K. Kim, J.P. Hong, W. Lee, S. Noh, C. Lee, S. Lee, J.I. Hong, Org. Electron 11 (2010) 1288–1295.
[13] J. Kwon, M.K. Kim, J.P. Hong, W. Lee, S. Lee, J.I. Hong, Bull. Korean. Chem. Soc. (2013) 1355–1360.
[14] R.F. Jin, Y.F. Chang, Phys. Chem. Chem. Phys. 17 (2015) 2094–2103.
[15] W. Che, W. Liang, J. Wang, G. Lin, G. Li, C. Han, X. Cui, D. Zhu, J. Mol. Sci. 29 (2013) 259–264.
[16] M. Mohamad, R. Ahmed, A. Shaari, S. Goumri-Said, J. Mol. Model 21 (2015) 27.
[17] L.Y. Zou, A.M. Ren, J.K. Feng, Y.L. Liu, X.Q. Ran, C.C. Sun, J. Phys. Chem. A 112 (2008) 12172–12178.
[18] W. Jiang, L. Duan, J. Qiao, G.F. Dong, L.D. Wang, Y. Qiu, Org. Lett. 13 (2011) 3146–3149.
[19] J. Ding, Q. Wang, L. Zhao, D. Ma, L. Wang, X. Jing, F. Wang, J. Mater. Chem. 20 (2010) 8126–8133.
[20] S. Paek, N. Cho, S. Cho, J.K. Lee, J. Ko, Org. Lett. 14 (2012) 6326–6329.
[21] P. Dutta, W. Yang, S.H. Eom, S.H. Lee, Org. Electron 13 (2012) 273–282.
[22] Z. Lu, C. Li, T. Fang, G. Li, Z. Bo, J. Mater. Chem. A 1 (2013) 7657–7665.
[23] A.L. Kanibolotsky, I.F. Perepichka, P.J. Skabara, Chem. Soc. Rev. 39 (2010) 2695–2728.
[24] K.R. Idzik, J. Frydel, R. Beckert, P. Ledwon, M. Lapkowski, C. Fasting, C. Müller, T. Licha, Electrochim. Acta. 79 (2012) 154–161.
[25] M.J. Frisch, G.W. Trucks, H.B. Schlegel, G.E. Scuseria, M.A. Robb, J.R. Cheeseman, G. Scalmani, V. Barone, B. Mennucci, G.A. Petersson, H. Nakatsuji, M. Caricato, X. Li, H.P. Hratchian, A.F. Izmaylov, J. Bloino, G. Zheng, J.L. Sonnenberg, M. Hada, M. Ehara, K. Toyota, R. Fukuda, J. Hasegawa, M. Ishida, T. Nakajima, Y. Honda, O. Kitao, H. Nakai, T. Vreven, J.A. Montgomery Jr., J.E. Peralta, F. Ogliaro, M. Bearpark, J.J. Heyd, E. Brothers, K.N. Kudin, V.N. Staroverov, T. Keith, R. Kobayashi, J. Normand, K. Raghavachari, A. Rendell, J.C. Burant, S.S. Iyengar, J. Tomasi, M. Cossi, N. Rega, J.M. Millam, M. Klene, J.E. Knox, J.B. Cross, V. Bakken, C. Adamo, J. Jaramillo, R. Gomperts, R.E. Stratmann, O. Yazyev, A.J. Austin, R. Cammi, C. Pomelli, J.W. Ochterski, R.L. Martin, K. Morokuma, V.G. Zakrzewski, G.A. Voth, P. Salvador, J.J. Dannenberg, S. Dapprich, A.D. Daniels, O. Farkas, J.B. Foresman, J.V. Ortiz, J. Cioslowski, D.J. Fox, Gaussian 09, Gaussian, Inc., Wallingford, CT, 2009 .
[26] D. Gudeika, A. Michaleviciute, J.V. Grazulevicius, R. Lygaitis, S. Grigalevicius, V. Jankauskas, A. Miasojedovas, S. Jursenas, G. Sini, J. Phys. Chem. C 116 (2012) 14811–14819.
[27] R.A. Marcus, Rev. Mod. Phys. 65 (1993) 599–610.
[28] R.A. Marcus, Annu. Rev. Phys. Chem. 15 (1964) 155–196.
[29] V. Lemaur, M. Steel, D. Beljonne, J.-L. Brédas, J. Cornil, J. Am. Chem. Soc. 127 (2005) 6077–6086.
[30] D.L. Cheung, A. Troisi, J. Phys. Chem. C 114 (2010) 20479–20488.
[31] D.P. McMahon, A. Trois, J. Phys. Chem. Lett. 1 (2010) 941–946.
[32] S. Di Motta, E. Di Donato, F. Negri, G. Orlandi, D. Fazzi, C. Castiglioni, J. Am. Chem. Soc. 131 (2009) 6591–6598.
[33] M.E. Köse, H. Long, K. Kim, P. Graf, D. Ginley, J. Phys. Chem. A 114 (2010) 4388–4393.
[34] K. Sakanoue, M. Motoda, M. Sugimoto, S. Sakaki, J. Phys. Chem. A 103 (1999) 5551–5556.
[35] M.E. Köse, W.J. Mitchell, N. Kopidakis, C.H. Chang, S.E. Shaheen, K. Kim, G. Rumbles, J. Am. Chem. Soc. 129 (2007) 14257–14270.
[36] N.E. Gruhn, D.A. da Silva Filho, T.G. Bill, M. Malagoli, V. Coropceanu, A. Kahn, J.L. Brédas, J. Am. Chem. Soc. 124 (2002) 7918–7919.
[37] B.C. Lin, C.P. Cheng, Z.Q. You, C.P. Hsu, J. Am. Chem. Soc. 127 (2005) 66–67.
[38] W. Huang, X. Zhang, L. Ma, C. Wang, Y. Jiang, Chem. Phys. Lett. 352 (2002) 401–407.
[39] M.S. Alexiou, V. Tychopoulos, S. Ghorbanian, J.H.P. Tyman, R.G. Brown, P.I. Brittain, J. Chem. Soc. Perkin. Trans. 2 (1990) 837–842.
[40] J. You, L. Dou, K. Yoshimura, T. Kato, K. Ohya, T. Moriarty, K. Emery, C.C. Chen, J. Gao, G. Li, Y. Yang, Nat. Commun. 4 (2013) 1446–1455.
[41] M. Lenes, G.A.H. Wetzelaer, F.B. Kooistra, S.C. Veenstra, J.C. Hummelen, P.W.M. Blom, Adv. Mater. 20 (2008) 2116–2119.
[42] S.E. Shaheen, C.J. Brabec, N. Serdar Sariciftci, Appl. Phys. Lett. 78 (2001) 841–843.
[43] M.M. Wienk, J.M. Kroon, W.J.H. Verhees, J. Knol, J.C. Hummelen, P.A. van Hal, R.J. Janssen, Angew. Chem. Int. Ed. 42 (2003) 3371–3375.
[44] P.v.R. Schleyer, N.L. Allinger, T. Clark, J. Gasteiger, P.A. Kollman, H.F. Schaefer III, P.R. Schreiners, Encyclopedia of Computational Chemistry, Chichester, UK, Wiley, 1998.